A Novel Probabilistic Path Loss Model for Simulating Coexistence Between 802.11 and 802.15.4 Networks in Smart Home Environments

Amr El-Keyi[†], Hamza Umit Sokun[†], Tu Ngoc Nguyen[‡],
Qiubo Ye[‡], Haiying Julie Zhu[‡], and Halim Yanikomeroglu[†]

[†] Department of Systems and Computer Engineering, Carleton University, Ottawa, Ontario.
[‡] Communications Research Centre, Ottawa, Ontario.

***Abstract*—In this paper, experimental measurements of the received signal strength in a smart home test bed are presented. The measurements are used to develop a topology-independent probabilistic indoor path loss model. The proposed path loss model adds a random loss component to the log-distance path loss model to account for wall penetration, reflection, scattering, and diffraction effects. The proposed model is incorporated into the network simulator ns-3 to simulate IEEE 802.11 and IEEE 802.15.4 networks. Our results indicate that the throughput of both networks degrades as the density of the nodes increases due to increasing the connectivity of the interference links.**

I. Introduction

Smart homes improve the security, safety, comfort level, and energy efficiency of houses [1]. Smart homes join all devices, such as door openers, thermostats, and light switches to a wireless network that enables them to communicate with each other and with the users. Smart home networking is one of the applications of Internet of Things (IoT) networks in which everyday physical devices are connected to the Internet using distinct identities to communicate with each other as well as with manufacturers and/or operators [2]. Key enabling wireless technologies for smart home networking include the IEEE 802.11 wireless local area network protocol and the IEEE 802.15.4 low power personal area network protocol. Both IEEE 802.11 and IEEE 802.15.4 operate in the 2.4 GHz license-free industrial scientific and medical (ISM) band, and hence they can interfere with each other. The problem is complicated due to the high transmission power of IEEE 802.11 compared to IEEE 802.15.4. With the increasing number of devices and systems operating in the ISM band, interference between these systems can be a serious concern.

Coexistence between IEEE 802.11 (Wi-Fi) and IEEE 802.15.4 (Zigbee) networks in the ISM band has been studied through both measurements and simulations [3], [4]. Simulation-based studies of wireless networks require simple path loss models that can capture indoor propagation effects such as attenuation, scattering, diffraction, and reflection with enough accuracy. Several empirical path loss models have been proposed for indoor environments, e.g., the one-slope model [5], the multi-wall-floor model [6], and the ITU indoor path loss model [7]. Similar to the free space path loss model, the above models utilize a log-distance term to model the path loss. Received signal strength (RSS) measurements are then utilized to evaluate additional path loss terms that correspond to wall and floor penetration losses and/or estimate the path loss exponent. Ray tracing has also been utilized to model indoor propagation effects. However, all the above approaches require knowledge of the electromagnetic properties of building walls and/or the topology of the building.

In this paper, we present an indoor probabilistic path loss model for smart homes that probabilistically accounts for additional path loss resulting from wall penetration, reflection, scattering, and diffraction effects. The proposed model does not require knowledge of the house topology or wall material. The probability of experiencing additional path loss depends only on the distance between the transmitter and the receiver. RSS measurements are collected in a testbed resembling a smart home environment and are used to estimate the parameters of the model using least-squares. We formulate the least-squares problem as a mixed integer conic program that can be solved using standard solvers. In addition, we describe a traffic measurement campaign to measure the throughput between different nodes in both IEEE 802.11 and IEEE 802.15.4 networks. Using the results of this campaign, we extract traffic modelling parameters of typical smart home applications. The proposed models are integrated into the network simulator ns-3 which is utilized to investigate the limits of coexistence between 802.11 and 802.15.4 devices as their number increases. Simulation results show that both density and data rate of interfering nodes have an important impact on the total throughput of both IEEE 802.11 and IEEE 802.15.4 networks.

The remainder of this paper is organized as follows. Section II presents the smart home test bed. Section III describes the proposed indoor path loss model. Network simulation results are provided in Section IV and conclusions in Section V.

Amr El-Keyi, Hamza Umit Sokun, and Halim Yanikomeroglu are with Carleton University, 1125 Colonel By Dr, Ottawa, ON, Canada, e-mails: amr.elkeyi@sce.carleton.ca, husokun@sce.carleton.ca, halim@sce.carleton.ca.

Tu Ngoc Nguyen, Quibo Ye, Haiying Julie Zhu are with the Communications Research Centre, 3701 Carling Avenue, Ottawa, ON, Canada, emails: tungoc.nguyen@canada.ca, qiubo.ye@canada.ca, haiying.zhu@canada.ca.

978-1-5386-3531-5/17/$31.00

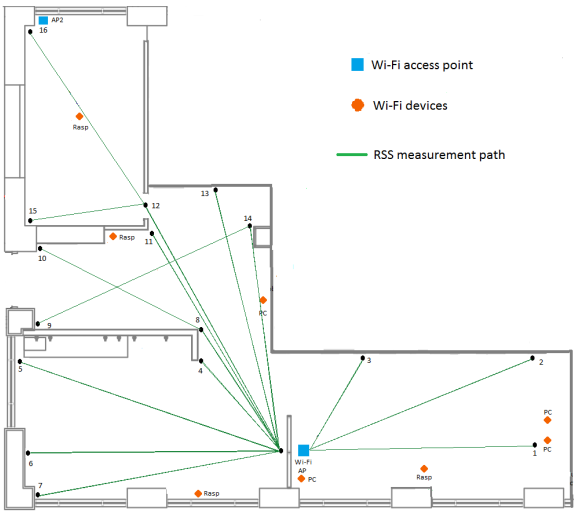

Fig. 1: Measurement routes and test bed layout.

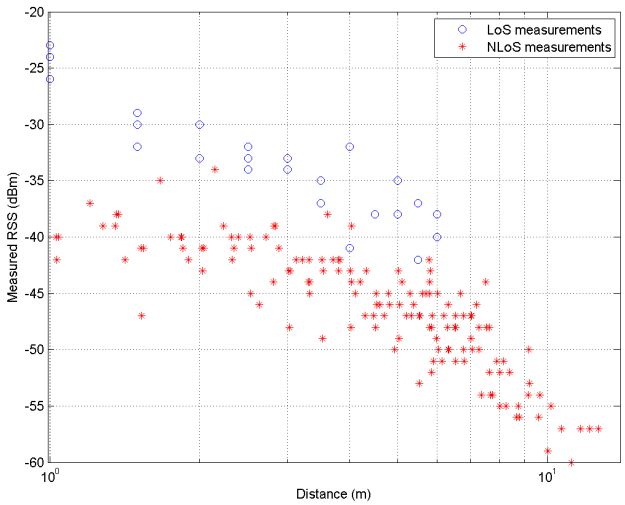

Fig. 2: Measured RSS versus distance using Wi-Fi.

II. RSS Measurement Test Bed

Fig. 1 shows the layout of Wi-Fi devices in the test bed that represents a typical smart home. The Wi-Fi channel was set to channel 1 corresponding to the center frequency of 2412 MHz. The second router acted as a second access point and was also set to use the same channel as the first router. The RSS of Wi-Fi was measured on sixteen different routes that cover most of the area of the test bed. Fig. 1 shows the measurement paths where the RSS was measured every half meter from the starting point to the end point of each route by the Wi-Fi receiver. Consumer routers ASUS RT-AC66 were selected for the Wi-Fi access points. The Wi-Fi routers were updated with open source firmware that allows the transmitted power to be set manually. The transmission power was fixed at 71 mW. The Wi-Fi receiver, a Raspberry Pi with Wi-Fi USB dongle, was used with the Linux software "Wavemon" that continuously polls the RSS value in dBm format. The RSS values were collected at each measurement point after a minimum of twenty seconds to ensure RSS stabilization.

At each measurement point in each of the sixteen routes, the average RSS was recorded. The collected RSS measurements were used to compute the path loss at different measurement points. Fig. 2 shows the measured RSS on all routes versus the distance between the first Wi-Fi router and the Wi-Fi receiver. The measurements corresponding to points with line-of-sight (LoS) connectivity to the router, i.e., points on measurement paths 1–3, are marked in blue while those corresponding to measurement points obstructed from the router are marked in red. We can see from this figure that non-LoS connectivity incurs an additional path loss causing further attenuation to the RSS. However, additional path loss can also occur in locations with LoS connectivity for example due to scattering, reflection, and diffraction. Furthermore, some points with non-LoS connectivity have relatively high RSS values.

Fig. 5 shows the power coverage for the test bed obtained using a commercial ray tracing software. The color scale bar indicates the strength of the power level from red (high) to deep blue (low). We can notice from this figure that due to scattering and reflection, some areas with non-LoS connectivity have relatively high RSS while others with LoS connectivity have low RSS. Although deterministic path loss models such as the multi-wall-floor model or the ITU indoor path loss model can capture path loss due to non-LoS connectivity, they do not capture the effects of reflection, diffraction, and scattering. In Section III, we use the collected RSS measurements to develop a probabilistic indoor path loss model for smart home environments. The path loss model is used later in Section IV to investigate the coexistence between 802.11 and 802.15.4 devices via simulations.

In addition to RSS measurements, we have conducted a throughput measurement campaign to capture salient features of Wi-Fi and IoT traffic in typical smart home environments. The network activities between clients and hosts were tested with a variety of network protocols and the network traffic was measured. For example, video applications were streamed by different protocols. Real Time Streaming Protocol (RTSP) was used by the Raspberry Pi. On the other hand, the MyFox camera device used the UDP protocol if the client was in the same home network or SKYPE protocol if the client was in an external network. Wi-Fi and ZigBee packets were captured by USB dongles. The traffic was monitored using "tcpdump" installed directly on the Wi-Fi router which was the main gateway of the 802.11 network. This program captured all network traffic between clients and hosts in the internal network or between internal and external networks. USB dongle sniffers were used to capture packets for the Zigbee protocol and the captured packets were saved to file in PCAP format for later processing. Wireshark was used for processing the captured packets due to its ability to support many protocols such as IEEE 802.11, IEEE 802.15.4, and Bluetooth. Fig. 3 shows the measured traffic of the 802.15.4-based water-leak sensor obtained from analyzing the captured packets using

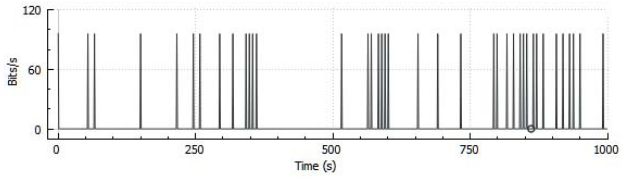

Fig. 3: Measured traffic for IoT-based water-leak sensor (bits/s).

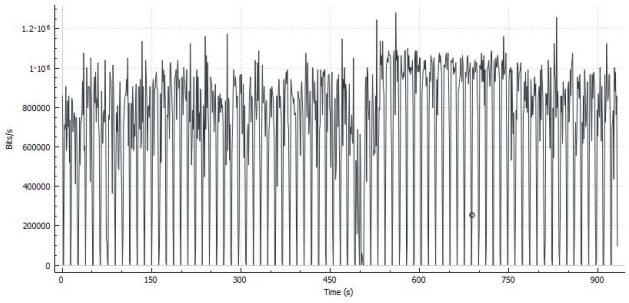

Fig. 4: Measured traffic for Wi-Fi UDP application (bits/s).

Wireshark. We can see from this figure that the 802.15.4 traffic can be characterized by the average rate of the packets and the packet size where the packet size is given by 96 Byte and the transmission rate of the sensor is 0.04 packet/sec. Fig. 4 shows the captured traffic for a typical 802.11 application running on the Raspberry Pi and transmitting UDP packets through the Wi-Fi access point to one of the personal computers. We can see from this figure that the traffic pattern resembles an on/off source. The traffic can be characterized by three parameters; the on time, the off time, and the data rate during transmission. In Section IV, the performance of the network is evaluated as the number of Wi-Fi and 802.15.4 nodes increases. In the simulation, the traffic of the simulated nodes is generated using the traffic models reported in this section.

III. Indoor Path loss Modelling

In this section, we develop a layout-independent probabilistic path loss model for smart homes using the collected measurements. The proposed model is based on the log-distance path loss model. A probabilistic attenuation component is utilized to model the additional path loss due to non-LoS connectivity, scattering, reflection, and diffraction. In particular, we model the path loss in decibel as

$$L(d) = L_0 + u(d)L_a + 10n\log(d) \tag{1}$$

where d is the distance between the transmitter and receiver in meters, L_0 is reference path loss at distance 1 m, n is the path loss exponent, $L_a \geq 0$ is the additional path loss, $u(d)$ is a binary random variable that indicates whether the transmitter receiver pair separated by a distance d experiences additional path loss or not, i.e., $\Pr\{u(d) = 1\} = p_a(d)$ and

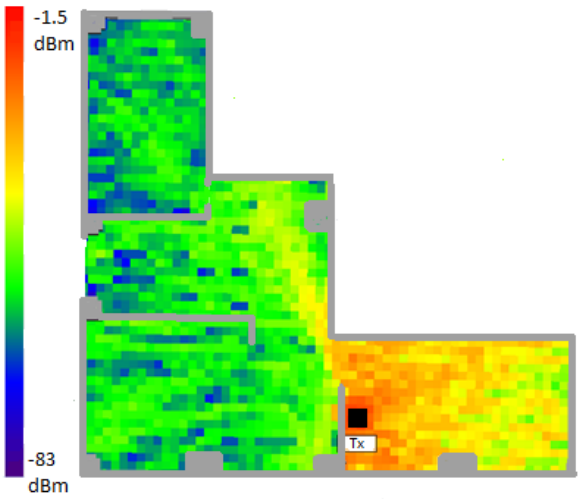

Fig. 5: Simulated RSS values using ray tracing.

$\Pr\{u(d) = 0\} = 1 - p_a(d)$. The parameters of the model are L_0, L_a, n, and $p_a(d)$. We utilize the results of the measurement campaign to estimate these parameters via least-squares fitting.

In order to include the effect of the additional path loss in the least-squares fitting problem, we associate the ith measurement with a binary indicator variable v_i, where $v_i = 1$ if the measurement point experiences additional path loss and $v_i = 0$ else[1]. Since we cannot determine beforehand whether a recorded measurement (d_i, L_i) experiences an additional path loss or not, we consider $\{v_i\}_{i=1}^N$ as unknown variables where N is the number of recorded measurements. Therefore, we pose the least-squares fitting problem as

$$\begin{aligned} \min_{L_0, L_a, n, \{v_i\}_{i=1}^N} \quad & \sum_{i=1}^{N} \left(L_i - (L_0 + v_i L_a + 10n\log(d_i))\right)^2 \\ \text{subject to} \quad & v_i \in \{0,1\}, \qquad \text{for } i = 1, \ldots, N. \end{aligned} \tag{2}$$

The above problem is a mixed integer nonlinear program. In order to solve this problem, we start by eliminating the product of the binary variables v_i and the continuous variable L_a in the objective function by substituting with $y_i = v_i L_a$, where y_i is a continuous variables, and adding the following constraints

$$y_i \leq \min\left\{\bar{L}v_i, L_a\right\} \tag{3}$$

$$y_i \geq \max\left\{L_a - \bar{L}(1 - v_i), 0\right\} \tag{4}$$

where $\bar{L}$ is an upper bound on L_a. In our problem, we have selected L_a from the measurement set as $L_a = \max_i L_i$. Since $L_a \geq 0$, we can easily verify that the constraints in (3)–(4) reduce to $y_i = 0$ when $v_i = 0$ and to $y_i = L_a$ when $v_i = 1$.

[1]The probability distribution of $u(d)$ will be obtained from the histogram of v_i via (6).

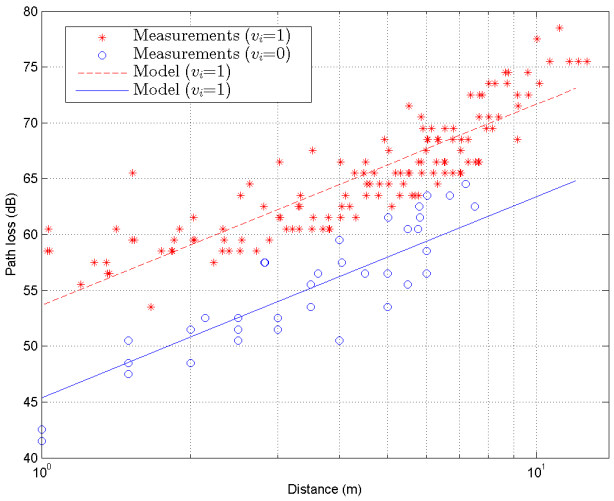

Fig. 6: Path loss versus distance.

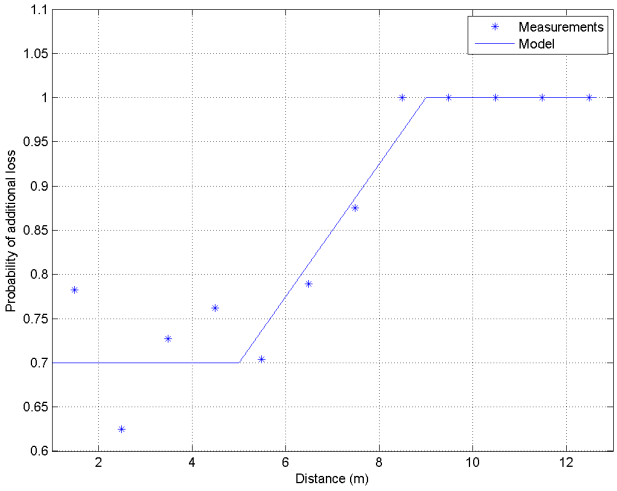

Fig. 7: Probability of additional loss versus distance.

Hence, we can write the optimization problem in (2) as

$$\min_{L_0,L_a,n,\{y_i,v_i\}_{i=1}^N} \quad \sum_{i=1}^{N} \left(L_i - (L_0 + y_i + 10n\log(d_i))\right)^2$$
$$\text{subject to} \quad v_i \in \{0,1\}, \qquad \text{for } i = 1,\ldots,N$$
$$(3) - (4) \tag{5}$$

which is a mixed integer conic program that can be solved using MOSEK. Fig. 6 shows the results of solving the optimization problem in (5) using the collected measurements. We can see from this figure that the solver can successfully classify the measurements into two sets using the indicator variables $\{v_i\}$. The returned values by the solver for the model parameters were $n = 1.8$, $L_0 = 45.4$ dB, and $L_a = 8.3$ dB.

In order to derive a model for the probability of additional loss, we divide the measurements into distinct sets$\{\mathcal{S}_i\}$. The ith set contains the measurements recorded at a distance $i \leq d < i+1$, i.e., the measurement distance is divided into non-overlapping bins of width 1 m. The center of the ith bin is located at $d_{c_i} = i + 0.5$ m. The probability of additional loss at d_{c_i} is computed from the measurements as

$$p_a(d_{c_i}) = \frac{1}{|S_i|} \sum_{v_i \in \mathcal{S}_i} v_i \tag{6}$$

where $|S_i|$ denotes the cardinality of S_i. Fig. 7 shows the values of $p_a(d_{c_i})$ obtained from processing the measurements in addition to a piecewise-linear empirical model given by

$$p_a(d) = \begin{cases} 0.7, & d \leq 5 \\ 0.7 + \frac{3}{40}(d-5), & 5 < d \leq 9 \\ 1, & d > 9 \end{cases} \tag{7}$$

that can be used to model the probability of additional path loss $p_a(d)$ at a distance d. The proposed model can provide a simple and accurate layout-independent approximation for indoor propagation in smart home environments.

IV. An Application: Simulating IEEE 802.11 and IEEE 802.15.4 Coexistence with NS-3

In this section, we investigate the limits of coexistence between IEEE 802.11 and IEEE 802.15.4 networks in the 2.4 GHz frequency band as the number of devices increases. We utilize the network simulator ns-3 in this study. The ns-3 simulator is well-known for providing high fidelity, packet-level models of Wi-Fi, LTE, and low-rate wireless personal area networks. The ns-3-laa project was launched to study coexistence between WiFi and LTE in the unlicensed 5 GHz band. The first phase of the project produced a new Wi-Fi Spectrum-based physical layer, enabling Wi-Fi and LTE devices to coexist on the same ns-3 simulation channel. We have extended the spectrum channel available in the ns-3-laa simulator to include support for the 2.4 GHz band allowing simultaneous simulation of IEEE 802.11 and IEEE 802.15.4 networks. We have also integrated the probabilistic path loss model presented in Section III to the ns-3-laa library.

We consider a scenario with several IEEE 802.11 nodes with a maximum transmit power of 20 dBm, and several IEEE 802.15.4 nodes with transmit power 0 dBm. We assume that the IEEE 802.15.4 nodes communicate in peer-to-peer mode. We also assume that the 802.11 network is deployed in infrastructure mode, in which there is a wireless access point with several attached clients. In this setting, the location of the access point is assumed to be fixed. The mobility model of IEEE 802.11 client nodes and 802.15.4 nodes is selected as random walk in an area of size 10×10 meters. In order to simulate the interference between the two networks, the 802.11 and 802.15.4 nodes are enforced to use channel 1 and channel 11 (both in non-beacon enabled mode), respectively. In the simulations of the IEEE 802.11 network, the data rate is fixed, and the modulation and coding scheme index is 31.

For the IEEE 802.11 network, we model the traffic of each flow (client to server) as an on-off application with the following parameters: packet size=1514 Byte, protocol=UDP,

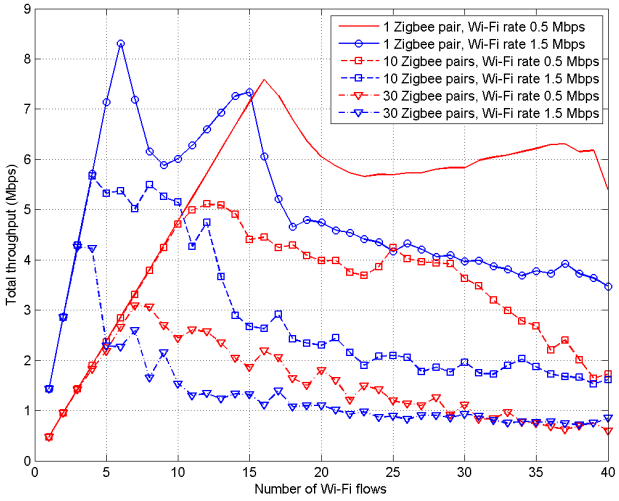

Fig. 8: Total Wi-Fi throughput with different number of Zigbee pairs.

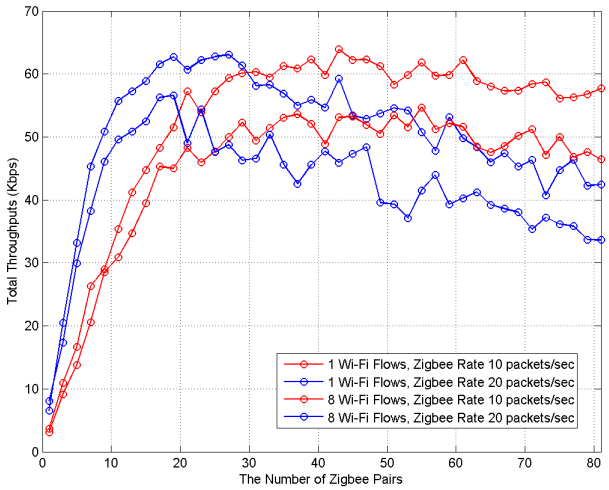

Fig. 9: Total Zigbee throughput with different number of Wi-Fi flows.

on time=1 sec, off time= 1 sec. In addition, different application data rates for simulations are considered. On the other hand, for the 802.15.4 network, we have developed a traffic source module and integrated it with ns-3. Using this module, 802.15.4 packets are generated at random arrival times with average arrival rate 10 packets/sec and packet size 101 Byte.

Fig. 8 shows the total throughput of IEEE 802.11 nodes versus the number of IEEE 802.11 flows. Each flow originates from one of the client nodes and is transmitted to a different client node through the access point. In this figure, we consider three network instances with 1, 10, and 30 pairs of 802.15.4 nodes. From this figure, it can be readily observed that the total throughput of IEEE 802.11 increases linearly as we increase the number of IEEE 802.11 flows until excessive interference among the 802.11 nodes leads to degrading the total throughput. The throughput degradation point depends on the number of interfering 802.15.4 nodes. In the presence of a single pair of IEEE 802.15.4 nodes, the total throughput starts to degrade when the number of IEEE 802.11 flows is around 17. However, in the presence of 10-pairs and 30-pairs of IEEE 802.15.4 nodes, the degradation starts earlier due to higher interference from 802.15.4 transmissions. Increasing the density of the nodes increases the probability of having interference links with high connectivity.

Fig. 9 shows the total throughput of IEEE 802.15.4 devices versus their number in the presence of interference from IEEE 802.11 devices. We can see from this figure that the decrease in the packet success rate due to collisions with the transmission of IEEE 802.11 and among IEEE 802.15.4 devices affects the total throughput of IEEE 802.15.4 network. We can see that the presence of IEEE 802.11 devices decreases the maximum achievable throughput of IEEE 802.15.4 devices. In addition, the number of IEEE 802.15.4 nodes that can be accommodated in the system without reducing the total throughput of the system is decreased.

V. Conclusion

We have developed a novel probabilistic indoor path loss model for smart home environments. The proposed model adds a probabilistic loss component to the log-distance path loss model to account for indoor propagation effects. We have integrated the proposed path loss model into the network simulator ns-3 to test the performance of 802.11 and 802.15.4 as the number of devices increases. Our results indicate that the throughput of both 802.11 and 802.15.4 networks are severely degraded due to interference. The degradation depends on the density of the nodes and the data rate of the traffic.

Acknowledgment

The authors would like to thank Hugh Dysart, Wayne Brett, Bobby Ho, Raymond Wu, and David Kidston, from the Communications Research Centre (CRC), Canada, for their contributions in building the smart home testbed and editing this manuscript.

References

[1] A. Zanella, N. Bui, A. Castellani, L. Vangelista, and M. Zorzi, "Internet of things for smart cities," *IEEE Internet Things J.*, vol. 1, pp. 22–32, Feb. 2014.

[2] K. Xu, Y. Qu, and K. Yang, "A tutorial on the internet of things: from a heterogeneous network integration perspective," *IEEE Netw.*, vol. 30, pp. 102–108, Mar. 2016.

[3] P. Dong, Z. Zhang, and F. Tong, "Experiment based analysis of ZigBee transmissions under severe Wi-Fi interference," in *Proc. IEEE Int. Conf. on Cyber Tech. in Autom., Control, and Intel. Sys.*, pp. 317–322, June 2014.

[4] L. Tytgat, O. Yaron, S. Pollin, I. Moerman, and P. Demeester, "Analysis and experimental verification of frequency-based interference avoidance mechanisms in IEEE 802.15.4," *IEEE/ACM Trans. Netw.*, vol. 23, pp. 369–382, Apr. 2015.

[5] A. Goldsmith, *Wireless Communications*. Cambridge: Cambridge University Press, 2005.

[6] M. Lott and I. Forkel, "A multi wall and floor model for indoor radio propagation," in *Proc. IEEE Veh. Tech. Conf.*, May 2001.

[7] J. Seybold, *Introduction to RF Propagation*. Hoboken, NJ: Wiley Interscience, 2005.